J Ther Eng, Vol. 10, No. 5, pp. 1390–1410, September, 2024

Journal of Thermal Engineering
Web page info: https://jten.yildiz.edu.tr
DOI: 10.14744/thermal.0000869

Review Article

A state-of-the-art review on thermo fluid performance of brazed plate heat exchanger for HVAC application

Madhu Kalyan Reddy PULAGAM[1], Sachindra Kumar ROUT[1,*], Sunil Kumar SARANGI[1]

[1]*Department of Mechanical Engineering, C. V. Raman Global University, Bidyanagar, Mahura, Bhubaneswar, Odisha, 752054, India*

ARTICLE INFO

Article history
Received: 29 February 2024
Revised: 25 June 2024
Accepted: 27 June 2024

Keywords:
CFD; Fluid Flow; Friction Factor; Heat Transfer; Plate Heat Exchangers

ABSTRACT

Plate heat exchangers have served various industrial applications for decades, with brazed plate heat exchangers (BPHE) emerging as preferred choices due to their favorable operating conditions. While extensive research has been conducted on flow patterns in gasketed plate heat exchangers, similar studies for *BPHE* have been lacking, given their analogous geometry. However, recent years have witnessed a surge in research focusing on single and multi-phase flow dynamics. Advancements in computational fluid dynamics *(CFD)* have furthered our understanding by providing insights into flow and heat transfer patterns, while also reducing the need for costly experimental tests of different geometries. This has facilitated the adoption of parametrization, bolstered by the feasibility and accuracy of numerical models. Nevertheless, substantial research remains to be undertaken to develop comprehensive models capable of integrating multiple geometric and flow parameters. This article examines existing research on *BPHE* and outlines potential areas for future exploration to address current research gaps.

Cite this article as: Pulagam MKR, Rout SK, Sarangi SK. A state-of-the-art review on thermo fluid performance of brazed plate heat exchanger for HVAC application. J Ther Eng 2024;10(5):1390−1410.

INTRODUCTION

Heat exchangers serve as crucial devices for transferring heat between a solid and a fluid medium or between two fluid mediums. From household refrigerators to thermal power plants, these versatile devices come in various forms, shapes, and sizes, catering to a wide range of applications. For over a century, heat exchangers have been integral components of refrigeration and air conditioning systems, as well as numerous industrial processes requiring heating, cooling, or isothermal operations. Compact heat exchangers are those heat exchangers which have a surface area to volume ratio of more than 700 m^2/m^3 for gasses and 300 m^2/m^3 for liquids They find extensive use in equipment where achieving a close temperature approach is essential. While several design methods, such as the Logarithmic Mean Temperature Difference (LMTD) method or the effectiveness – Number of transfer units (*ε-NTU)* method, are prevalent in the literature, determining the heat transfer coefficient and pressure drop remains a persistent challenge. Over the years, research efforts have yielded established correlations for many commonly encountered geometries, providing valuable insights into heat exchanger

***Corresponding author.**
*E-mail address: sachindra106@gmail.com

This paper was recommended for publication in revised form by Editor-in-Chief Ahmet Selim Dalkılıç

Published by Yıldız Technical University Press, İstanbul, Turkey

performance. However, ongoing research continues to explore specialized cases, indicating that we may just be scratching the surface of the field's potential.

The plate heat exchanger, credited to Dr. Richard Seligman in 1923, comprises a series of plates stacked atop each other, each featuring embossed corrugations. These corrugations, angled to create channels when the plates are flipped and stacked, facilitate local turbulence even at low Reynolds numbers upon fluid entry. The ends of the exchanger are sealed using either gaskets or brazing, ensuring the separation of hot and cold fluids via a lining of gasket material or brazed metal at the entry and exit ports. When designing for specific applications, existing geometries can be leveraged. Heat transfer rates can be controlled by adjusting plate quantities, altering flow patterns, or modifying plate arrangements, allowing for tailored design without necessitating the creation of an entirely new device. A classification of plate heat exchangers is depicted in Figure 1.

Gasketed plate heat exchangers (G*PHE*s) stand as the most prevalent type among plate heat exchangers. These devices feature a gasket lining between stacked corrugated plates, ensuring the integrity of the liquid channels by preventing leaks into the surrounding environment and between individual fluid streams, as illustrated in Figure 2. The primary domain of application for G*PHE*s lies within the food industry, particularly in milk processing plants. Here, they play a pivotal role in cooling fluids like yoghurt and processed milk. Additionally, they find widespread use as chillers across various industries due to their superior effectiveness compared to traditional shell and tube or tubular heat exchangers, all while occupying significantly less space.

In *BPHE*s, gaskets are replaced with brazed joints to enhance plate strength. By brazing the contact points of the corrugations between two plates, the unsupported length of the load-bearing corrugation significantly reduces, thereby improving the pressure limits and overall operating conditions of the exchanger. Moreover, brazing eliminates the

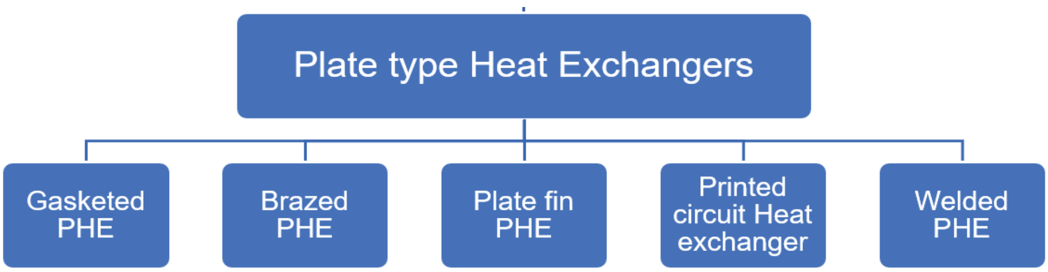

Figure 1. Classification of plate heat exchangers (PHE).

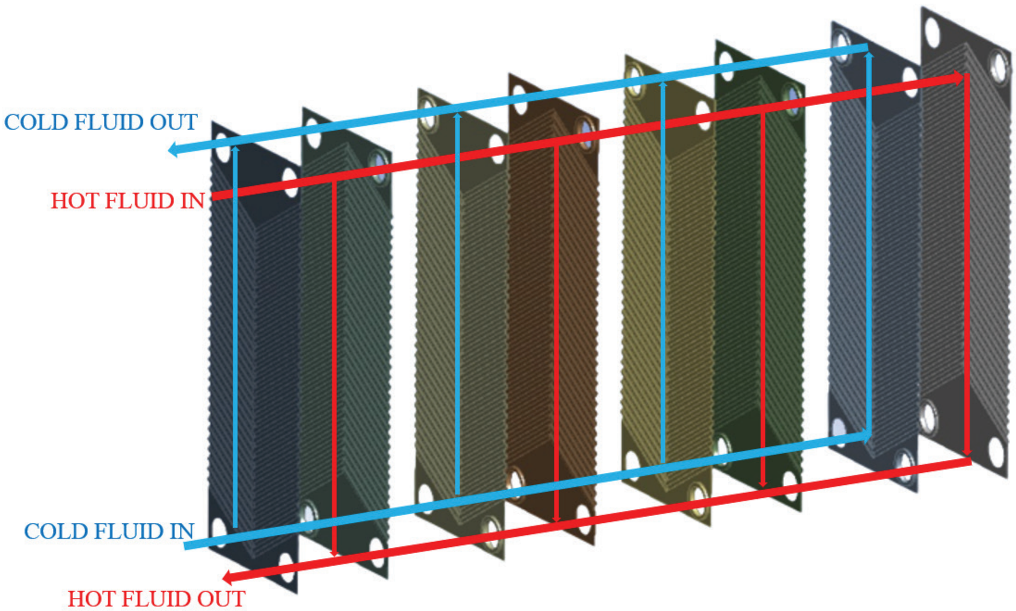

Figure 2. General flow pattern in plate heat exchangers.

need for certain support structures necessary for Gasketed Plate Heat Exchangers *(GPHEs)*, making *BPHE*s lighter and more compact for the same heat transfer capacity. This reduction in size and weight is particularly advantageous in applications where space is limited or weight constraints are a concern.

This article provides a comprehensive summary of research conducted on *BPHE*s. While the focus is primarily on *BPHE*s, certain sections also include references to studies involving gasketed plate heat exchangers (G*PHE*s) due to their similar flow behavior. The content is organized into distinct sections based on the type of study conducted, such as single-phase flow analysis, numerical simulations, etc. As a result, certain articles may be referenced in multiple sections to ensure thorough coverage of relevant research findings. The following Table 1 contains the layout of the article with a brief description.

CHRONOLOGY

The plate heat exchanger, invented by Dr. Richard Seligman in 1923 [1], saw significant advancements in its design and construction over the ensuing decades. In 1968, Butt [2] filed a patent outlining methods for constructing and repairing plate heat exchangers. Subsequently, in the early 1970s, Alfa Laval revolutionized the technology by introducing *BPHE*. By brazing the joints and eliminating gaskets, Alfa Laval enhanced the efficiency and durability of plate heat exchangers. The exploration of plate heat exchangers by researchers initially paved the way for investigations into *BPHE*. In the 1980s, pioneering works by Thonon [3], Focke et al. [4], Shah [5] etc., were among the pioneers of research in this field, providing insights into the working of plate heat exchangers. These studies yielded correlations for key parameters such as the friction factor (*f*) and Colburn factor (*j*), elucidating the effects of varying geometric and flow parameters. Further innovations continued to emerge

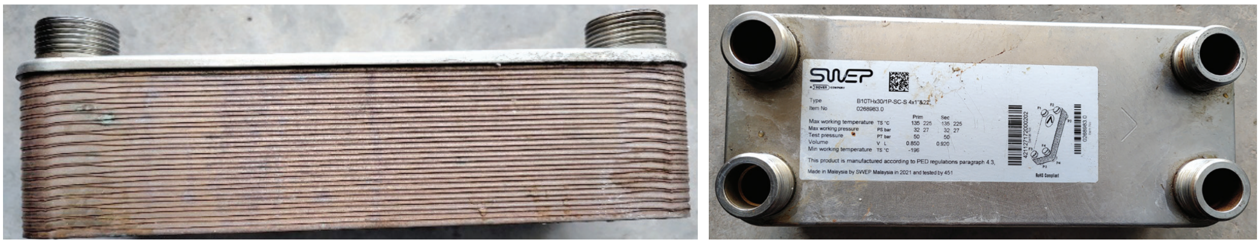

Figure 3. Brazed plate heat exchanger.

Table 1. Layout of the article

Section	Title	Description
1	Introduction	A brief introduction to the compact heat exchangers and brazed plate heat exchangers
2	Chronology	This section gives an overview of the timeline of the research conducted over the years since the invention of the plate heat exchanger.
3	Study of heat transfer and flow friction *PHE*nomena	Plate heat exchangers offer higher heat transfer rates than traditional shell and tube heat exchangers. This section glances over the studies that observed the heat transfer and flow patterns inside the heat exchangers
4	Study of single-phase flow in brazed plate heat exchanger	This section covers the studies done on the heat exchangers carrying the fluid that doesn't change its phase throughout the study
5	Study of two-phase flow in brazed plate heat exchanger	Most refrigerants are studied in brazed plate heat exchangers owing to their application in HVAC industries. The majority of the work has been done on two-phase flows in a brazed plate heat exchanger. This section deals with the research done over the years in two-phase flow
6	Numerical studies on brazed plate heat exchangers	A small part of the community studied the heat exchangers using simulation software such as ANSYS Fluent. This section deals with the studies that observed the heat exchangers virtually by simulating the flow conditions inside them in a computer
7	Correlations developed over the years	Correlations are bound to be developed based on the experimental and numerical data available to the researchers. This section has the correlations developed over the years based on the data collected by the respective studies

throughout the decade. In 1985, Allison [6] patented a procedure for simplifying maintenance by removing end bars. Additionally, in 1989, Fuerschbach et al. [7] secured a European patent detailing a construction method that incorporated brazed joints to eliminate unnecessary structural components, thereby reducing the weight of the heat exchanger. These developments underscored a concerted effort to enhance the efficiency, maintenance, and structural integrity of plate heat exchangers.

As plate heat exchangers gained traction as evaporators and condensers in the refrigeration industry, Yam et al. [8] emerged as pioneers in the late 1990s, providing correlations for the Nusselt number and friction factor. Subsequent years saw a surge in research focusing on the effects of geometry, with scholars delving deeper into these aspects. In the year 2001, William and Glen Hubman [9] a novel construction method for *BPHE*, employing metal gaskets to enhance structural integrity. The following year, Heil et al. [10] introduced and patented another construction method for plate heat exchangers, further expanding the technological repertoire in the field. Between 2000 and 2010, several *CFD* studies were conducted on plate heat exchangers, exploring phenomena such as fouling [11] and investigating the impact of corrugations [12] and corrugation angle [13] on pressure drop and heat transfer. Notably, in 2013, Otahal and Hofer [14] patented a plate heat exchanger featuring a turbulence generator, aiming to optimize heat transfer efficiency. A few years later, Krantz [15] from Alfa Laval Corporate patented innovative gasket and plate designs that purported to enhance heat transfer performance in plate heat exchangers. These developments underscored ongoing efforts to refine and innovate within the realm of plate heat exchanger technology.

The pertinent literature on *BPHE* began to emerge around 1995, with Bogeart and Boles [16] conducting a study on the performance of an industrial prototype *BPHE*. In 2000, Palmer et al. [17] investigated the effects of flammable refrigerants in *BPHEs*, shedding light on safety considerations in their application. Subsequently, Han et al. [18] explored R410A evaporation in *BPHEs* in 2003, providing insights into refrigerant behavior within these exchangers. Longo et al., continued this line of research, focusing on the evaporation and condensation of various refrigerants in *BPHE*s since 2007. Their work has significantly contributed to understanding the thermal performance of *BPHE*s across different operating conditions. Gullapalli [19] utilized a combination of *CFD* and experimental data to optimize *BPHE* designs, culminating in a doctoral thesis in 2013. Further publications [20] and [21] by Gullapalli and others have built upon this research, refining *BPHE* design methodologies. Due to their compactness and high heat transfer rates, *BPHE*s have found application in carrying nanofluids and as evaporators in Organic Rankine Cycle (ORC) systems. Barzegarian et al. [22] investigated the heat transfer and pressure drop of TiO_2 nanofluids in *BPHE*s in 2015, while Teng et al. [23] examined the characteristics of carbon-based nanofluids in *BPHE*s. Recent years have witnessed contributions from researchers such as Desideri et al. [24], Gullapalli [21], Kim and Kim [25] and Nematollahi et al. [26] towards integrating *BPHEs* into ORC systems, expanding the scope of their applications in energy conversion processes.

Through the analysis of the optical and thermal behavior of particulate media, it is clear that photo-thermal energy conversion is important to not only the solar thermal systems but also to the electric power generation and solar chemical technology. This research investigates the effects of nanoparticle suspensions (water/TiO_2 nanoparticle suspension) at different particle concentrations on the radiative properties and radiative transfer phenomena. The effect and contribution of the TiO_2 nanoparticles on the radiative properties in the UV-Vis-NIR wavelength ranges are observed, which have a significant impact for the solar thermal applications.

Study of Heat Transfer and Flow Friction *Phe*nomena

The study of heat transfer and flow friction phenomena in *BPHE* is crucial due to their compactness and high heat load capacities in small sizes. The intricate channels formed between the plates play a significant role in achieving these high heat transfer rates. While most studies have historically focused on gasketed plate heat exchangers, the similarities in design between gasketed and *BPHE* allow findings from these studies to be applied to *BPHE*s.

In the early days of *BPHE* research, limited experimental studies provided valuable insights into the flow patterns responsible for heat transfer and pressure drop characteristics. However, with the advent of computational fluid dynamics *(CFD)* software such as ANSYS Fluent, visualization of flow patterns has become much more accessible. This technological advancement has enabled researchers to gain a better understanding of how the geometric features of *BPHE*s impact their performance.

Overall, the combination of experimental studies and *CFD* simulations has greatly contributed to advancing our knowledge of heat transfer and flow friction phenomena in *BPHE*s, facilitating the design and optimization of these highly efficient heat exchangers.

Study of flow patterns and flow friction phenomenon

Dović and Švaić [12] investigated flow patterns and flow friction in *BPHE* to gain deeper insights into their performance characteristics. Employing visual aids, the researchers examined flow patterns within *BPHEs* utilizing two heat exchangers with chevron angles of 28° and 61°. Transparent plates specifically designed for this study allowed observation of a die inserted into the flow at various Reynolds numbers, enabling detection of any changes in direction due to geometric factors. The flow was characterized into two components: the longitudinal component, which flowed alternately along adjacent plates, and the furrow component, representing flow along the corrugations or furrows.

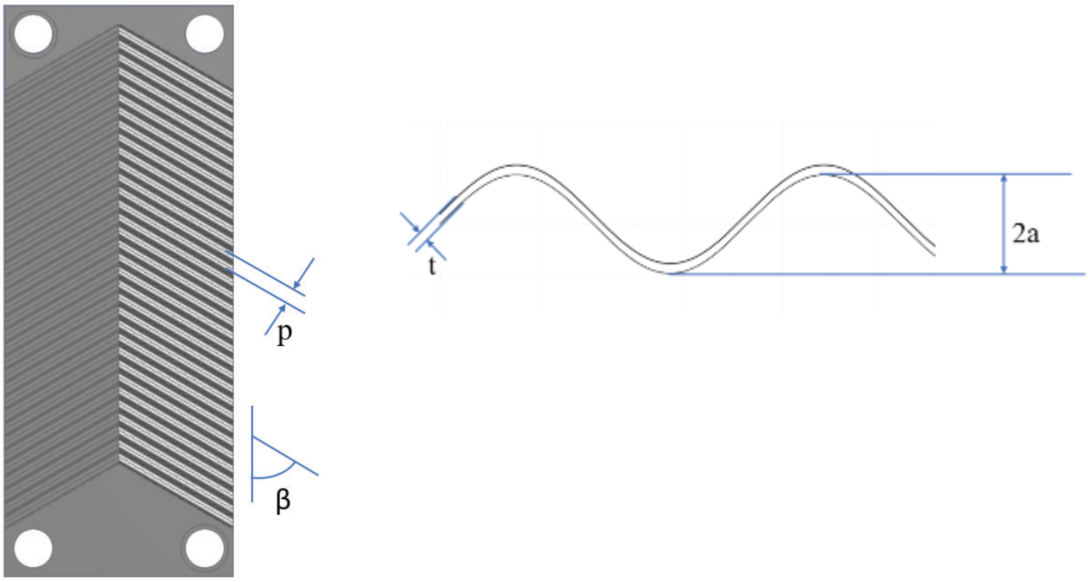

Figure 4. Schematic of the plate geometry.

Results depicted in Figure 5 illustrated that as the ratio of amplitude to the length of the corrugation increased, the furrow component became more dominant in the flow. At low Reynolds numbers, the longitudinal component prevailed due to insufficient velocity to induce mixing among sub-streams. However, at higher chevron angles and Reynolds numbers, although the longitudinal component remained dominant, increased mixing among streams enhanced heat transfer efficiency. Furthermore, the study highlighted the influence of chevron angle and aspect ratio on heat transfer performance. Lower amplitude-to-length ratios were favored at lower chevron angles, where the longitudinal component played a more significant role, leading to improved performance. Conversely, higher aspect ratios proved beneficial at higher angles, promoting enhanced heat transfer efficiency. These findings underscored the importance of geometric parameters in optimizing heat transfer in *BPHEs*.

Study of heat transfer characteristics

While research on flow patterns was limited, investigations into the impact of corrugations and associated geometry on heat transfer were more prevalent. Focke et al. [4] delved into the effect of chevron angle on pressure drop and heat transfer coefficient. Ten machined plates with angles ranging from 0° to 90° were stacked for the study. It was observed that at a 90° angle, flow separation occurred even at low Reynolds numbers (Re), leading to reduced pressure

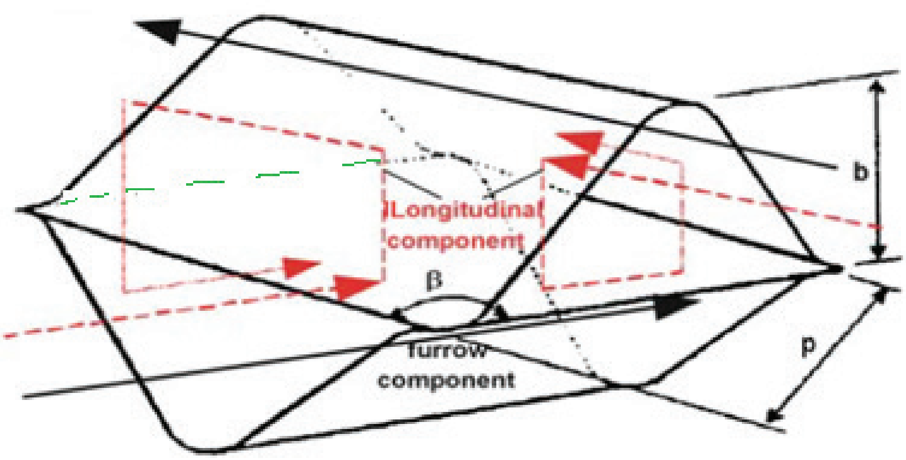

Figure 5. Longitudinal and furrow components [From Dović and Švaić [12] with permission from Author].

drop and heat transfer. Additionally, the study highlighted that the ends of plates contributed minimally to pressure drop and heat transfer calculations.

Kandlikar and Shah [27] developed effectiveness formulae for various flow patterns and configurations of multi-pass plate heat exchangers (*PHE*s), using a computer program to calculate temperature effectiveness. With increasing number of plates, the influence of end plates diminished gradually, stabilizing after 40 plates without significant changes in temperature effectiveness. Galeazzo et al. [28], a four-channel *PHE* was modeled using *CFD*. They compared the results with experimental data and a 1D plug flow model. Parallel and counter-flow arrangements were simulated and experimented with in this study. Due to the omission of ambient heat losses in *CFD*, the values of heat load were consistently higher than actual experimental values. The 1D model proved to be unreliable because of the requirement of numerous experimental runs for adjusting the correlations. The correlations were accurate with the experimental data.

Muley and Manglik [29] conducted experimental studies on turbulent flow heat transfer and pressure drop in plate heat exchangers, noting discrepancies in previous studies regarding the use of power law curve fit equations and variations in error percentages. Their experiments utilized plate combinations with chevron angles of 30° and 30°, 30° and 60°, and 60° and 60°. Iterative multiple linear regression analysis was employed to formulate correlations for the waterside, serving as calibration equations for the experimental setup. Results indicated that Nusselt number (Nu) increased with chevron angle, suggesting intensified swirl flows. Despite some disagreements with previous studies, it was concluded that flow and thermal patterns were primarily influenced by geometric differences like amplitude and pitch. Additionally, it was noted that Focke et al. [4] had not considered correction factors for viscosity variations in their Nusselt number equations. The area enlargement factor, reflecting the ratio of actual surface area to projected area, significantly impacted heat transfer, with deeper corrugations promoting swirl flow and effective area enlargement. Ultimately, heat transfer enhancement of up to 2.8 times that of a flat plate channel was achieved, with correlations for Nusselt number and friction factor presented based on the study's data.

Study of Single-Phase Flow in Brazed Plate Heat Exchanger

Expanding upon the foundation established by single-phase flow studies in gasketed plate heat exchangers, research in *BPHE* has evolved. Correlations of *f* and *Nu* from Kumar [30], Focke et al. [4], and others have been instrumental in validating and refining experimental results. While brazed plate heat exchangers are typically utilized as evaporators or condensers, scenarios exist where both sides experience single-phase flow. Consequently, ongoing research in single-phase flow aims to establish correlations for friction factor and Nusselt number, facilitating broader applicability across various studies in the field.

Blomerius and Mitra [31] conducted numerical investigations on convective heat transfer and pressure drop in wavy ducts angled at 45° and 90°, considering the influence of unsteadiness. Grijspeerdt et al. [11] employed *CFD* modelling to analyze the hydrodynamics of plate heat exchangers (*PHE*s) with a 56° chevron angle, primarily focusing on applications in the milk processing industry due to fouling concerns. Similarly, Galeazzo et al. [28] modelled a four-channel *PHE* using *CFD*, comparing results with experimental data and a 1D plug flow model. Jain et al. [13] simulated small-sized *PHE*s, studying flow maldistribution effects and comparing results with experimental data. Kanaris et al. [32] utilized optimization techniques to design a *PHE* with V-shaped corrugations, achieving optimal performance by minimizing the obtuseness of corrugations and reducing channel width. They highlighted the dominance of secondary flows in corrugations, leading to increased heat transfer augmentation through flow separation and reattachment.

Han et al. [33] conducted numerical simulations and provided optimized results for single-phase turbulent flow in a plate heat exchanger with sinusoidal corrugations, utilizing a different optimization technique from Kanaris et al. [32]. They also presented a formula for the area enlargement factor, similar to Shah's textbook approach. Simulations covered chevron angles of 30° and 60° across a wide range of Reynolds numbers. Fernandes et al. [34] observed low Reynolds number flow in chevron plates for highly viscous fluids, noting increased flow tortuosity and resistance with reduced corrugation angles. They introduced a coefficient '*K*', derived from the shape factor and tortuosity coefficient, equivalent to the product of the Fanning friction factor and Reynolds number, suitable for laminar flow analysis using the Hagen-Poiseuille formula. Khan et al. [35] investigated single-phase heat transfer in plate configurations with varying chevron angles (30°/30°, 60°/60°, 30°/60°) and Reynolds numbers ranging from 500 to 2500. Results indicated a Nusselt number increase of 4 to 9 times compared to flat plate *Nu*, depending on the corrugation angle configuration, at a given Reynolds number.

Manigandan et al. [36] experimentally observed the counter and parallel flow characteristics in a brazed plate heat exchanger. Different flow rates of water in the hot and cold sections were used along with various inlet temperatures. No significant correlations were used or derived from the data and only the outlet temperatures and heat loads were plotted for parallel and counter flow. Gurel et al. [37] introduced a lung-patterned design onto plates, mimicking the efficient heat transfer capabilities of the human pulmonary system. This intricate design aimed to leverage the rapid heat exchange properties of human lungs, with flow velocity highest at pattern ends. Increasing pattern branches stabilized pressure drop while enhancing heat transfer efficiency. Compared to a referenced plate heat exchanger (*PHE*), the lung-patterned design demonstrated a significant 71% increase in heat transfer and a notable 67.8% reduction in pressure drop. Suggestions included rounding branch ends for further pressure drop reduction and energy savings. Fernández-Seara et al. [38] explored the use of offset strip fins in *BPHE*, analyzing flow and heat transfer characteristics for water-ethylene glycol solutions.

Cremasachi et al. [39] explored fouling performance in *BPHE*s used in cooling towers and air conditioning condensers, using four heat exchangers with 30° and 63° angles. Lower angles exhibited higher fouling and pressure drop due to settling calcium carbonate, with pressure drop nearly 200% higher. Kim and Park [40] compared two *BPHE*s with similar chevron angles but different hydraulic diameters, finding similar performance parameters despite Nusselt number variations, suggesting excess heat transfer increased pressure drop. Jin and Hrnjak [41] investigated the impact of end plates in frame plate and *BPHE*, noting their significance, especially with fewer plates and improved contact points. Li and Hrnjak [42] continued the study on end plate effects, conducting a theoretical analysis and developing an iterative model to compensate for their impact on heat transfer, incorporating insights from literature, and numerical, and analytical models.

Wu and Ju [43] replaced plate-fin heat exchangers with *BPHE* in four LNG processes and optimized cases to assess process flow and economic performance parameters. Zhong et al. [44] examined *BPHE* performance at low Reynolds numbers (5 to 50) through experimental and numerical analyses, establishing correlations for f. Observations revealed that increased angle and spacing correlated with higher friction factors. Jafari et al. [45] simulated three *BPHE* geometries, focusing on corrugation profile modifications and brazing joint presence. While the last geometry proved most accurate, its results lacked validation above 60°, with existing correlations unable to predict f and Nu effectively. Ham et al., [46] explored LiBr solution usage in *BPHE*s, proposing new Nu and f correlations from experiments conducted in a Vapor Absorption Refrigeration System, with one side handling a weak solution and the other a strong solution.

Nanofluids, containing nanoparticles in a liquid, exhibit enhanced heat transfer compared to the base fluid. Barzegarian et al. [22] investigated TiO_2-water nanofluid in a *BPHE*, noting an increase in convective heat transfer coefficient with nanoparticle concentration. Teng et al. [23] explored carbon-based nanofluids in laminar flow *BPHE*, finding higher heat exchange capacity and lower pumping power for lower-concentration nanofluids. Fazeli et al. [47] optimized MWCNT-CuO nanofluid heat transfer in *BPHE*, noting a 39.27% thermal conductivity increase. Mehrarad et al. [48] reported a 94% Nusselt number increase and a 12.87% friction factor increase for the same nanofluid. Additionally, they emphasized the potential of nanofluids for enhancing heat transfer efficiency in *BPHE*s, especially in applications where compactness and high heat transfer rates are crucial, such as in refrigeration and HVAC systems. Gungor [49] compared energy consumption between H-type and L-type *BPHE*s, finding superior heat transfer and pressure drop for the H-type, especially at higher flow rates. This research underscores the importance of nanofluids in optimizing heat transfer performance and energy efficiency in *BPHE* applications, with potential implications for various industries and systems requiring efficient heat exchange. In addition to the existing research, Pulagam et al. [50] investigated the impact of Al_2O_3-water nanofluid in a brazed plate heat exchanger. Utilizing *CFD* modelling, they assessed the nanofluid's influence on heat transfer and friction factor across a variety of *BPHE* designs. Their findings indicated minimal changes in friction factor and Nusselt number, a crucial observation considering factors such as economic feasibility and fluid preparation complexities. Jalili et al. [51] investigated the use of a curved rectangular fin in a double-pipe heat exchanger carrying nanofluid. An improvement of 81% to 85% in efficiency was observed. Another work by Jalili et al. [52] investigated the thermo-hydraulic performance of a non-continuous baffle with different helix angles and hybrid nanoparticles. It was observed that increasing the helix angle decreases the heat transfer coefficient by almost 50%. Both of the works were influential in the usage of nanofluids in heat exchangers. Kaplan et al. [53], Bousri et al. [54], Aouanouk et al. [55], Zhu et al. [56] have also made significant contributions.

The study of single-phase flow in plate heat exchangers has laid a solid foundation for understanding fluid behavior and optimizing heat transfer performance. Various studies have investigated the effects of geometric parameters, such as corrugation angle and amplitude, on friction factor and Nusselt number correlations. These findings have been crucial in designing efficient heat exchangers for diverse applications. Moving forward, the focus shifts to exploring two-phase flow phenomena, including boiling and condensation, which are essential for applications like refrigeration, HVAC systems, and power generation. By building upon the insights gained from single-phase flow studies, researchers aim to further enhance the performance and efficiency of plate heat exchangers in handling multiphase fluid flows.

Study of Single-Phase Flow in Brazed Plate Heat Exchanger

The increasing use of *BPHE* as evaporators/condensers has led to extensive research on the behavior of various refrigerants within these systems. While some researchers focused on specific refrigerants like R134a [8] or R410A [18], Giovanni A. Longo stands out for his comprehensive exploration of numerous refrigerants since the CFC ban. Longo's research, spanning multiple refrigerants, has been pivotal in developing correlations for evaporation and condensation within *BPHE*. His meticulous documentation and extensive data collection have provided valuable insights into refrigerant behavior in these systems, shaping our understanding of their performance and efficiency. Subsequent sections will delve into Longo's work, highlighting the range of refrigerants studied and the comparative analyses conducted

Yan et al. studied R-134a evaporation [8] and condensation [57] in a plate heat exchanger. They found that R-134a, being a potential CFC replacement, was explored due to its ban. Unlike prior studies focusing on smooth pipes, this was the first examination of R-134a in a plate heat exchanger. Using a 60° corrugation angle heat exchanger, they observed linear relationships between vapor quality and condensation heat transfer coefficient. Despite minimal impact from mass flux variations, condensation heat transfer was notably higher in plate heat exchangers compared to circular pipes. Pressure drop increased with heat flux but showed little change beyond a certain threshold. For evaporation, the heat transfer coefficient increased exponentially with vapor quality and mass flux, with pressure drop rising accordingly. Overall, these findings shed light on the unique behavior of R-134a in plate heat exchangers. Hsieh and Lin [58] studied R410A evaporation, while Kuo et al. [59] focused on its condensation, addressing the lack of two-phase heat transfer data in plate heat exchangers. Their experiments revealed increasing heat transfer coefficients with vapor quality and mass flux, with notable effects in condensation. System pressure minimally affected heat transfer, contrasting with R-134a. The studies offered insights into R410A behavior, essential for its adoption as a refrigerant replacement.

Longo (and Gasparella) examined R410A's vaporization [60] and condensation [61] in a brazed plate heat exchanger, revealing a significant sensitivity to heat flux and outlet conditions. Confirming nucleate boiling dominance using the Lockhart-Martineli parameter used by Palm and Claesson [62], the observation was validated. Frictional pressure drop was correlated to kinetic energy per unit volume with a mean deviation of around 8.5%. Condensation displayed weak sensitivity to saturation temperature, with mass flux doubling enhancing the heat transfer coefficient by up to 30%. A fitted correlation for frictional pressure drop yielded a mean deviation of approximately 22%. Longo (and Gasparella) explored R134a's vaporization [63] and condensation [64] in the same brazed plate heat exchanger used in prior studies, echoing trends seen with R410A, albeit with slight deviations. Heat transfer coefficients were compared using previous correlations [54] and [55], with a mean deviation of around 8.2% and 12.3% respectively. The Webb model predicted heat transfer coefficients during condensation's forced convection. They further investigated R236fa's vaporization [65] and condensation [66], noting similar trends to R410A and R134a. R410A displayed higher coefficients than R134a and R236fa during vaporization but similar ones during condensation, with significantly lower frictional pressure drop. Vaporization of R236fa was dominated by convective boiling, while the other two were by nucleate boiling.

Longo et al. [67] conducted a comparative study, akin to [68], assessing heat transfer coefficients and pressure drops in a heat exchanger for R600a, R290, and R1270 as HFC refrigerant alternatives. Notably, R290 demonstrated similar performance to R22 in heat transfer with a 50% lower pressure drop. R1270 exhibited higher heat transfer coefficients than R600a and R290, with lower pressure drops. Further studies on superheating during condensation

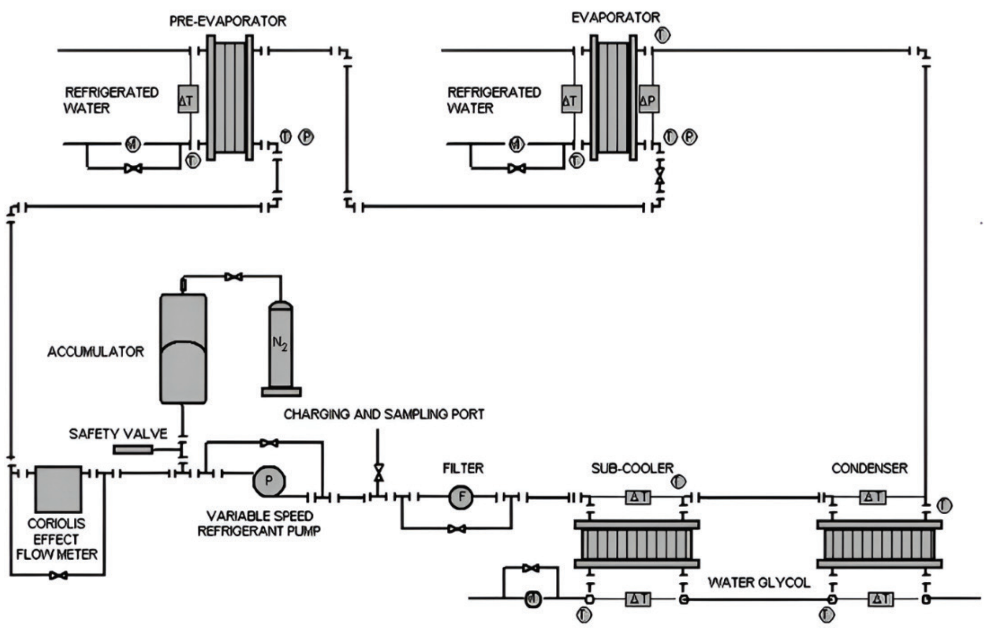

Figure 6. Experimental setup used for *BPHE* testing [From Longo and Gasperalla [60], with permission from Elsevier.]

[69], [70] revealed increased heat transfer coefficients but unchanged pressure drops. These findings indicate a consistent trend in heat transfer coefficient dependencies on saturation pressure, outlet conditions, mass flux, and heat flux, consistent with Longo's earlier work. Additionally, nucleate boiling was confirmed using previously employed equations, with IR thermography analysis shedding light on heat transfer surface areas affected by vapor superheating. R1234yf [71], studied as a potential R134a replacement, exhibited slightly lower heat transfer coefficients (6%-10%) and pressure drops (10%-18%) compared to R134a.

Longo et al. investigated R1234ze(E) condensation [72] and vaporization [73], demonstrating trends consistent with their previous studies. Condensation exhibited a heat transfer coefficient 4%-6% lower and a 10% higher pressure drop than R134a. Vaporization comparisons with R1234yf and R134a revealed similar heat transfer coefficients but slightly higher pressure drops. Longo et al. [74, 75] developed computational models for boiling and condensation in *BPHE* using data collected over the years. These models categorized refrigerants into HFC and HC, HFO types. Nucleate boiling was dominant in some, while convective boiling prevailed in others. Correlations for heat transfer coefficients in nucleate and convective boiling were provided, along with a model for superheating. For condensation, models were developed for laminar and forced convection regimes, with correlations showing mean absolute deviations of around 20% and less than 16%, respectively, compared with experimental data.

Longo et al. [76] examined R152a for condensation, noting its potential as a replacement for R134a in large chillers. Results mirrored those of previous refrigerants tested, with a transition to forced convection condensation at a mass flux of 15 kg/m2s and a notable increase in heat transfer coefficient with doubled mass flux. R152a exhibited higher heat transfer coefficients than R290, R134a, and R1234ze(E), making it suitable for large chiller applications due to its low GWP. Additionally, the vaporization of R32 [77] was studied, revealing similarities in trends with R410A [60] but with lower heat transfer coefficients (20%-30%) and higher pressure drops (30%-40%). This was attributed to R32's lower reduced pressure compared to R410A, highlighting the importance of limiting superheat to maintain stable operation. Longo et al. [78] explored the vaporization and condensation behaviors of R404A, contrasting its performance with potential substitutes R290 and R1270. With R404A facing replacement due to its high GWP, comparisons were made under similar experimental conditions. Vaporization data showed a maximum 15% mean deviation when compared with existing models. R290 and R1270 demonstrated higher condensation heat transfer coefficients (25%-45%) with similar pressure drops, transitioning to forced condensation around 20 kg/m2s mass flux. IR thermography analysis revealed no dry-out during vaporization, suggesting R290 and R1270 as promising alternatives for R404A in refrigeration. In recent years, Longo et al. [79] explored the boiling characteristics of low GWP refrigerants R1234ze(Z) and R1233zd(E) under similar experimental setups. R1234ze(Z) exhibited higher heat transfer coefficients (17%-22%) and lower frictional pressure drops (7%-32%) compared to R1233zd(E), attributed to its superior thermophysical properties. IR thermography confirmed convective boiling dominance for both refrigerants, with outlet vapor superheating degrading average boiling heat transfer coefficients. Experimental data validated author-proposed models [68]. Additionally, Longo et al. provided local heat transfer coefficients for R32 and R410A [77], [80], showing fair agreement with Longo et al.'s correlations [74], [75]. They also presented local boiling and condensation heat transfer coefficients for R290 and R1270, concluding their performance to be intermediate between R404A and R410A.

Han et al. [18] conducted experiments to investigate the evaporation characteristics of R410A and R22 in various geometric configurations of *BPHE*, varying chevron angles and pitches. Results showed that as mass flux increased, so did the heat transfer coefficient, with a corresponding decrease in chevron angle. Decreased chevron angles led to longer flow times, while the average heat transfer coefficient decreased with rising evaporation temperature. Convective heat transfer prevailed, particularly in high-vapor-quality regions. Pressure drop increased with decreasing evaporation temperature, notably in lower chevron angle heat exchangers, and differed among the *BPHE*s with increasing vapor quality. Compared to R22, R410A exhibited 10%-30% lower pressure drop and 0%-15% higher heat transfer coefficients, suggesting its suitability as a replacement. In another study, Claesson [81] aimed to rectify potential errors in estimating the heat transfer coefficient in *BPHE*s based on previous work. Through theoretical analysis and comparison with experimental data, Claesson proposed a correction factor to enhance the accuracy of predicting heat transfer coefficients. Assumptions like negligible pressure drop and nucleate boiling were employed to simplify the derivation, yielding a correction factor deemed insignificant for moderate to high logarithmic mean temperature differences. The study affirmed the reliability of the logarithmic mean temperature difference method in predicting heat transfer coefficients in *BPHE*s.

Hayes et al. [82] explored carbon dioxide (CO_2) as a potential refrigerant for *BPHE* due to its high-pressure limits. Using custom *BPHE*s, they investigated single-phase and two-phase (condensation) flow of CO_2, maintaining superheat and sub-cool under 5°C. Pressure loss considerations included gravity effects, estimating a total loss of about 1.5 times the inlet velocity head. Friction factor correlations were provided for both single-phase and two-phase flow, with uncertainties below 3% and 10%, respectively. Muthuraman [83] analyzed *BPHE* performance with three chevron angle configurations (20°, 35°, and 45°), observing decreasing heat transfer coefficients with increasing chevron angle. Higher vapor quality led to increased heat transfer coefficients due to elevated turbulence levels, with frictional pressure drop rising with mass flux and vapor quality but decreasing with condensation temperature and chevron angle. A comparison of R410A and R22 showed heat transfer coefficient ratios ranging from 0.8 to 1.1 for different cases.

Mancin et al. [84] examined partial condensation of R32 while Rossato et al. [85] investigated flow boiling of R32 in *BPHE*s. For partial condensation, various inlet superheating levels were tested, revealing heat transfer coefficient ratios independent of mean vapor quality at 15 kg/m^{2}s, increasing with superheating at 20 kg/m^{2}s, and consistent trends at 40 kg/m^{2}s. In flow boiling, heat transfer coefficients increased with mass flux and heat flux but decreased with outlet vapor quality, influenced by nucleate and convective boiling at high heat fluxes. Pang et al. [86] assessed *BPHE* performance in a Joule-Thomson cooler with mixed refrigerant, highlighting the impact of the recuperative heat exchanger. Despite mass transfer resistance decreasing with heat flux during convective condensation, its fraction in overall heat transfer resistance increased. Forced convective boiling exhibited similar trends. The cooler took 100 minutes to reach 127 K from an ambient temperature of 294.4 K, with overall heat transfer coefficients ranging from 38.3 to 362.5 W/m^{2}K. Exergy efficiency varied from 54.2% to 85.7%.

Raveendran and Sekhar [87] investigated the performance of a water-cooled *BPHE* as a condenser in a domestic refrigeration system, comparing it with typical air-cooled condensers. Results showed significant improvements in energy efficiency, with the water-cooled *BPHE* reducing compressor work by 24%-28% and increasing coefficient of performance by 52%–68%. Energy consumption was also reduced by 21%-27%, with R290/R600a consuming 8.6% less energy than R134a. Palmer et al. [17] explored the heat transfer performance of flammable refrigerants in *BPHE*s, developing a common correlation. Taboas et al. [88] studied ammonia water mixture evaporation in a *BPHE*, finding that heat transfer coefficients varied with mean vapor quality and mass flux. Mutumba et al. [89] proposed new correlations for heat transfer in water to water and water to R1233zd(E) *BPHE*s across a range of Reynolds numbers.

Li and Hrnjak [90] utilized infrared (IR) cameras to examine two-phase regions and refrigerant maldistribution within *BPHE*s, subsequently validating their findings with experimental data. Their follow-up research [91] highlighted the detrimental impact of maldistribution on heat exchanger performance, attributed to discrepancies in heat transfer coefficients between superheated and two-phase regions. Li [92] further explored this phenomenon, investigating its implications for system control. They also visually analyzed two-phase refrigerants in inlet headers, while Navarro-Peris et al. [93] conducted similar maldistribution studies. Li and Hrnjak [94] extended their investigation to single-phase flow, developing numerical and mechanistic models [95] to estimate these effects, with computational fluid dynamics *(CFD)* models proving more accurate. Will et al. [96] conducted a thermal analysis using infrared thermography on *BPHE*, while Zendehboudi et al. [97] explored CO_2 refrigerants at supercritical states, observing Nusselt number increases with buoyancy force. Sadeghianjahromi et al. [98] studied chevron angle effects on heat transfer and pressure drop, employing the k-ε realizable model for turbulent simulations. Salman et al. [99] examined saturation flow boiling of R290 in *BPHE*s with offset strip fins, yielding findings akin to Longo et al. [66] but with numerical differences due to plate configurations.

Gullapalli [100] developed a simulation program for Organic Rankine Cycle systems utilizing *BPHE*, offering design and performance modes for cost minimization and efficiency optimization, respectively. The program integrates thermal, hydraulic correlations, and refrigerant properties to ensure robust simulations. Meanwhile, Desideri et al. [24] investigated flow boiling and pressure drop in such systems using R245fa and R1233zd. They found that heat transfer coefficients decreased at 0.5–0.6 vapor quality due to local dry-out, with nucleate boiling dominating. Pressure drop decreased at higher saturation temperatures but increased with vapor quality, validated by previous studies and correlated well with existing models. Kim and Kim [25] investigated the efficacy of a brazed plate heat exchanger *(BPHE)* with a metal foam insert in an Organic Rankine cycle (ORC) setup. The modified heat exchanger demonstrated up to 2.3 times higher overall heat transfer coefficients compared to conventional *BPHE*s, despite increased pressure drop. Operating with R245fa, the brazed foam plate heat exchanger (*BFPHE*) exhibited lower outlet qualities and superheat temperatures than *BPHE*s. Despite its smaller size, *BFPHE* showed remarkable performance, with heat transfer rates ranging from 75 kW to 108 kW, 82% to 198% higher overall heat transfer coefficients, and higher frictional pressure drops compared to *BPHE*s. Nematollahi et al. [26] explored the application of brazed metal-foam plate heat exchangers (*BMPHE*s) in compact ORC systems. Utilizing water as the working fluid, *BMPHE*s demonstrated increased pressure drops and power densities compared to *BPHE*s, with efficiency gains of at least 1% and slightly enhanced power output, suggesting their suitability for compact *ORC* setups. Imran et al. [101] investigated the flow boiling characteristics of R245fa in a brazed plate heat exchanger *(BPHE)* for Organic Rankine Cycle systems. Testing different chevron angles, mass fluxes, vapor qualities, and heat fluxes, they observed that the heat transfer coefficient peaked at a vapor quality of 0.45 and decreased thereafter due to dry-out. Additionally, higher chevron angles and saturation temperatures correlated with increased heat transfer coefficients, affirming nucleate boiling as the dominant phenomenon. Frictional pressure drop was found to increase with vapor quality but decrease overall.

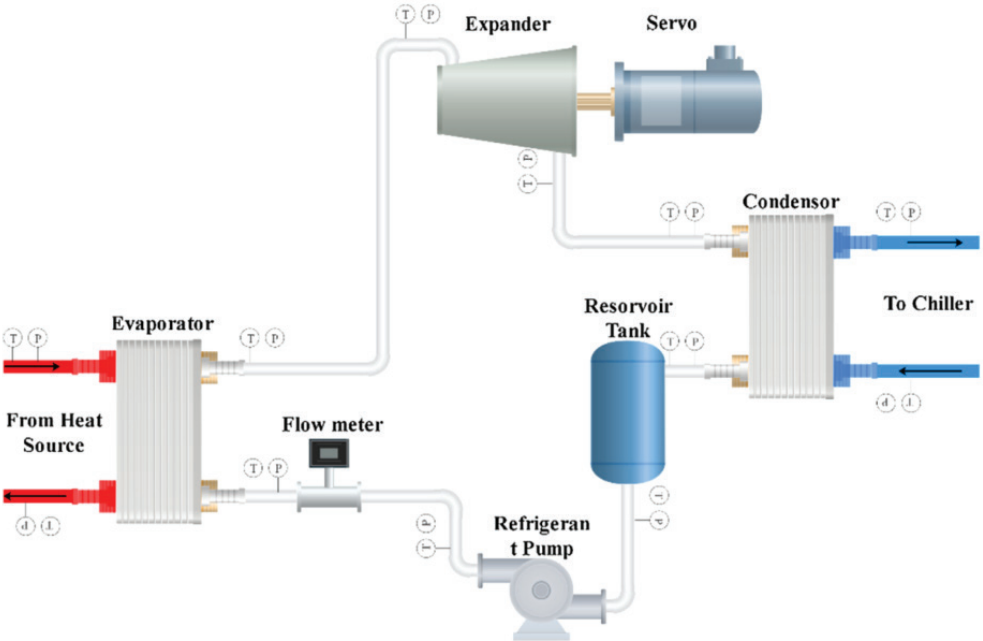

Figure 7. Schematic of ORC setup with BPHE [From Nematollahi et al. [26], with permission from Elsevier.]

Wu et al. [102] examined CO2 frosting and clogging in a *BPHE* during natural gas liquefaction, proposing *BPHEs* as alternatives to multi-pass plate-fin heat exchangers. They identified a CO_2 concentration threshold of 5000 ppm for clogging, significantly higher than plate-fin heat exchangers' 50 ppm. Implementing a stainless-steel filter, they mitigated clogging effects, enabling stable operation below 135 K and 3 MPa pressure. Through simulation and optimization, they achieved a 14.7% reduction in exergy loss, facilitating the design of compact LNG plants. Shon et al. [103] explored the condensation behavior of R1233zd(E) in a brazed plate heat exchanger *(BPHE)*, noting increasing heat transfer coefficients with higher heat and mass fluxes. While pressure drop remained relatively stable with varying heat flux, mean vapor quality exhibited a linear relationship with both heat transfer coefficient and pressure drop. Higher condensation pressure led to decreased heat transfer coefficients and pressure drop, necessitating new correlations due to differing refrigerant properties. Lee et al. [104] investigated the heat transfer and pressure drop of R-1233zd(E) and R-1234ze(E)/R32 in a *BPHE*. R-1233zd(E) showed potential as a replacement for R-245fa, with heat transfer coefficients primarily influenced by mass flux and vapor quality. Conversely, R-1234ze(E)/R32 demonstrated varied heat transfer behavior based on composition ratio, with optimal ratios meeting GWP regulations. Developed correlations provided insights into heat transfer and pressure drop characteristics for various refrigerant compositions.

Studies examining two-phase flow in *BPHE* offered valuable insights into their thermal performance across diverse operating conditions. Investigations by Gullapalli [24], Longo et al. [55] and others shed light on the heat transfer and pressure drop characteristics in single-phase flow, laying the groundwork for understanding fluid behavior in *BPHEs*. Building upon this foundation, studies by Shon et al. [103] and Lee et al. [98] delve into the complexities of two-phase flow, elucidating the impact of factors such as heat and mass fluxes on heat transfer coefficients and pressure drop. These findings underscore the critical role of both single-phase and two-phase flow phenomena in optimizing *BPHE* performance for various applications in refrigeration and energy systems.

Numerical Studies on Brazed Plate Heat Exchangers

Transitioning from experimental investigations to numerical studies, computational models offer a means to further explore and optimize *BPHE* designs. Through numerical simulations, researchers can analyze fluid dynamics, heat transfer mechanisms, and pressure distribution within *BPHEs* under a wide range of operating conditions. This approach enables the prediction of performance metrics such as heat transfer coefficients and pressure drop, facilitating the design of more efficient and reliable heat exchangers for diverse industrial applications at, comparatively, very low costs.

Kho and Muller-Steinhagen [105] delved into the fouling mechanisms, focusing on calcium sulfate precipitation, within Flat plate heat exchangers from Alfa Laval. Their experimental setup involved dissolving soluble salts containing calcium components in distilled water to facilitate calcium sulfate precipitation. Analyzing five heat exchanger specimens revealed the dominance of fouling near gaskets, attributed to low velocities at gasket walls and substantial deposits in the wake of longer distributors. Complementary *CFD* simulations, employing the *k-ε* model for its robustness and computational efficiency, provided valuable insights into flow patterns. While *CFD* results reasonably matched experimental findings, limitations of the *k-ε* model hindered the visualization of recirculation zones. Addressing this, the study recommended smoothing corners near ports to mitigate recirculation and minimize fouling in these regions.

Grijspeerdt et al. [11] employed *CFD* modelling to investigate the hydrodynamics of Plate Heat Exchangers (*PHE*) featuring a 56° chevron angle, focusing on applications within the milk processing industry where fouling is a significant concern. Their study, which built upon previous 1D flow models incorporating fouling effects, revealed that the influence of the inlet was limited to a short distance. Consequently, the length of the test specimen was adjusted accordingly, aligning with *CFD* predictions. This research laid a crucial groundwork for understanding fouling phenomena in *PHE* systems used in milk processing. In a related study, Galeazzo et al. [28] utilized *CFD* to model a four-channel *PHE*, comparing results with experimental data and a 1D plug flow model. The *k-ε* turbulence model with enhanced wall treatment was used with the model having one million nodes. Their investigation, encompassing both parallel and counter-flow arrangements, demonstrated the superiority of 3D *CFD* models over 1D counterparts in accuracy, despite the increased computational demands. This highlights the efficacy of 3D *CFD* simulations in capturing complex flow behavior and optimizing *PHE* designs.

Grigore et al. [106] explored the impact of plate number on plate heat exchanger (*PHE*) performance, considering configurations ranging from 3 to 10 plates in a 1-pass counter-flow arrangement. Utilizing the low-turbulent Reynolds k-ε model, they found that cold-water stream temperature increased with plate number, with even-numbered configurations exhibiting a faster temperature rise due to an additional hot channel. Interestingly, the effectiveness plateaued for configurations with 9 or 10 plates, indicating diminishing returns beyond this point. Fernandes et al. [34] defined a unit cell for *PHE* simulation, incorporating various geometric elements. Jain et al. [13] employed the *k-ε* realizable model with non-equilibrium wall conditions to simulate small-sized *PHE*s, validating results against experimental data. Meanwhile, Han et al. [33] optimized single-phase turbulent flow in *PHE*s with sinusoidal corrugations using the *k-ω SST* model, demonstrating good agreement with experimental validation by Khan et al. [35]. Muthuraman [83] utilized a simplified *CFD* model with the *k-ε* approach to gain insights into flow characteristics, acknowledging the need for further validation against experimental data to refine predictions and enhance accuracy.

Gullapalli [19, 20] worked on *CFD* and Experimental studies on *BPHE* in collaboration with a company (SWEP), which manufactures *BPHE* for his doctorate at the University of Lund, Sweden under the guidance of Sunden [107]. Single phase, condensation, and evaporation heat transfer were studied with a proper comparison of correlations from the previously available literature. The influence of channel parameters, fluid properties, and flow characteristics were explained in detail. Various available discretization methods, models, methods for designing a heat exchanger, linear and nonlinear regression models for the calculation of constants in empirical correlations, and optimization of those constants were discussed in detail. In the end, a generalized rating method was developed along with a one-dimensional discretization scheme which was integrated into the software for SWEP. Special cases, for example, where the saturation temperature crossed in the grid during two-phase flow, were studied and grid independence tests were conducted for selective cases. Additional software tools are used to optimize the empirical constants. The data from the software narrowed down the design parameters for the simulation because the design software does not have the correlations linking the effect of geometries on the performance of the heat exchanger. The performance-geometry correlations would be or could be developed from experimental data along with the validated numerical data from the simulations since the number of experiments can be limited because of various factors. A brief overview of the *CFD* models, mesh generation methods, wall treatment functions, and boundary conditions was given in the document. After various parametric studies using different configurations and models, it was determined that the Shear Stress Transport (*SST*) turbulence model predicted the results with the best accuracy given the hardware limitations. Experimental Data from SWEP International AB along with model-specific *CFD* analysis data was used to derive the correlations for water and water/glycerin mixture. No exact correlation was given as it must have been a proprietary right of the company, but some generalized equations for the Darcy friction factor and Nusselt number for single- and two-phase flows were given, including some corrections for multi-pass flow. A discretized rating method for trans-critical CO_2 gas cooler calculations and non-phase change processes with significant fluid property variation, along with the minimum resolution required for discretized calculations were also reported in great detail. Evaporation and condensation heat transfer for various refrigerants were also observed and reported upon experimental investigation and the step-wise rating method was also discussed. The author acknowledged the need to improve the generalized correlations. Gullapalli and Sunden [20] also used *CFD* to analyze pressure drop and heat transfer patterns in *BPHE* and validated the results against experimental data. A $y+$ value of less than 2 was maintained in this simulation study while using the *RNG k-ε* model, the *SST* model, and the Lunder-Reece-Rodi Isotropization of Production Reynolds stress model were used. For high mesh quality domains, it was concluded that the choice of the turbulence model made very little difference to the results. The data from the *CFD* was within 15%-20% of the error of the experimental data, which was good enough to predict data for other configurations.

Sevilgen and Bayram [108] conducted both experimental and numerical analyses of a brazed plate heat exchanger, where the full-scale heat exchanger was modelled and simulated using the *SIMPLE* algorithm and *k-ε* model. The numerical results closely matched the experimental findings within a 10% error margin for both parallel and counterflow configurations. Lonis et al. [109] utilized a brazed plate heat exchanger to harness cold energy from liquid nitrogen, aiming to optimize industrial energy usage. Simplified *CFD* geometries were employed, focusing on safe operating conditions by identifying potential freezing points for water. Anti-freezing agents were incorporated into simulations to determine the minimum water velocity for safe operation. Gurel et al. [37] performed *CFD* analysis using the Standard *k-ε* model. Pulagam et al. [50] applied periodic boundary conditions in their simulations, employing water and Al_2O_3-water nanofluid as working fluids. By calculating the nanofluid properties separately and introducing them as a separate fluid, the simulation complexity was reduced. The laminar and *SST k-ω* models were utilized for laminar and turbulent flow simulations, respectively.

Numerical studies on *BPHE* have been extensive and diverse, covering various aspects such as heat transfer, pressure drop, and flow characteristics. Researchers have utilized computational fluid dynamics *(CFD)* simulations to analyze single-phase and two-phase flows, as well as to investigate fouling and optimize energy usage. Studies have employed different turbulence models, meshing techniques, and boundary conditions to simulate *BPHE* performance accurately. Additionally, correlations derived from numerical simulations have been compared with experimental data, demonstrating good agreement and providing valuable insights for design and optimization. Despite challenges such as computational cost and complexity, numerical studies continue to contribute significantly to our understanding of *BPHE*s and pave the way for further advancements in the field.

Correlations Developed Over the Years

Correlations play a pivotal role in advancing research on *BPHE,* with potential applicability to gasketed plate heat exchangers due to their similar geometrical configurations. While correlations derived from gasketed plate heat exchangers can offer initial estimates for *BPHE*s with some error analysis, they provide valuable insights for new researchers in the field. However, generalizing correlations for estimating Nusselt number and friction factor remains challenging due to the significant influence of geometrical parameters. Unlike shell and tube heat exchangers, where correlations can be more easily adapted, the complex geometry of *BPHE*s complicates this task. Although numerous equations have been proposed by various authors, the economic constraints of experimental analysis limit the exhaustive exploration of all *BPHE* configurations by individual research teams. While numerical simulations offer a potential solution for developing generalized equations, their computational cost poses a challenge, leading to the proliferation of diverse correlations over time.

Focke et al. [4] and Kandlikar and Shah [27] have given too many correlations to summarize in this article. Focke et al. [4] have performed experiments with various chevron angles and gave different correlations for each case. Kandlikar and Shah [27] gave the correlations for effectiveness for each combination of plate arrangement. Martin [110] gave the correlation (Eq. 1 - 3) based on the data and correlations of existing studies.

$$Nu = 0.122Pr^{1/3}\left(\frac{\eta}{\eta_w}\right)^{1/6}\left[\xi\, Re^2\, sin(2\beta)\right]^{0.374} \quad (1)$$

$$\Delta p = \frac{\xi\, Re^2\, L_p \eta^2}{2d_h^3 \rho} \quad (2)$$

$$h_w = 19677\left[\frac{\Delta P}{1bar}\sin(2\beta)\right]^{0.374} \quad (3)$$

Yan et al. [8, 57] gave the correlations for the water side (Eq. 4) of the test heat exchanger as well as the refrigerant side for evaporation (Eq. 5-7) and condensation (Eq. 8-9) of R134a.

$$Nu_w = 0.2121\, Re^{0.78}\, Pr^{1/3}\left(\frac{\mu_m}{\mu_{wall}}\right)^{0.14} \quad (4)$$

For evaporation:2000<*Re*<10000

$$Nu_r = 1.926Pr_l^{1/3}Bo_{eq}^{0.3}\, Re^{0.5}\,\left[(1 - X_m) + X_m\left(\frac{\rho_l}{\rho_g}\right)^{0.5}\right. \quad (5)$$

$$f_{tp}Re^{0.5} = 6.967 \times 10^5 Re_{eq}^{1.109} \text{for } Re_{eq} < 6000 \quad (6)$$

$$f_{tp}Re^{0.5} = 6.967 \times 10^5 Re_{eq}^{1.109} \text{for } Re_{eq} \geq 6000 \quad (7)$$

For condensation: 2000<*Re*<10000

$$Nu = 4.118Re_{eq}^{0.4}Pr_l^{1/3} \quad (8)$$

$$f_{tp}\, Re^{0.4}\, B_0^{-0.5}\left(\frac{p_m}{P_C}\right) = 94.75Re_{eq}^{-0.0467} \quad (9)$$

Muley and Manglik [29] different correlations (Eq. 10 - 12) based on the chevron angle and area enlargement factor.

For $30 \le Re \le 400$, $30° \le \beta \le 60°$

$$Nu = 0.44 \cdot \left(\frac{\beta}{30}\right)^{0.38} \cdot Re^{0.5} \cdot Pr^{1/3}\left(\frac{\mu}{\mu_w}\right) \tag{10}$$

For other $Re > 1000$:

$$Nu = C_1(\beta)\, Re^{p_1(\beta)}\, Pr^{1/3}\left(\frac{\mu}{\mu_w}\right)^{0\cdot 14} \tag{11}$$

$$f = C_2(\beta) Re^{p_2(\beta)} \tag{12}$$

for $Re \ge 1000$, $30° \le B \le 60°$, $\phi = 1 \cdot 29$

$$C_1(\beta) = 0.2668 - 0.006967^{\beta} + 7.244 \times 10^{-5}\beta^2$$
$$C_2(\beta) = 2.917 - 0.1277\beta + 2.016 \times 10^{-3}\beta^2$$
$$P_1(\beta) = 0.728 + 0.0543\, sin\left(\frac{\pi\beta}{45}\right) + 3.7$$
$$P_1(\beta) = -\left[0.2 + 0.0577\, sin\left(\frac{\pi\beta}{45}\right) + 2.1\right]$$

For $Re \ge 10^3$, $30° \le \beta \le 60°$, $1 \le \phi \le 1 \cdot 5$

$$C_1(\beta) = \left[0.2668 - 0.006967^{\beta} + 7.244 \times 10^{-5}\beta^2\right]2 \times [20.78 - 50.94\phi^{+41.16}\phi^2 - 10.51\phi^3]$$
$$C_2(\beta) = [2.917 - 0.1277\beta + 2.016 \times 10^{-3}\beta^2] \times [5.474 - 19.02\phi + 18 \cdot 93\phi^2 - 5.341\phi^3]$$
$$P_1(\beta) = 0.728 + 0.0543\, sin\left(\frac{\pi\beta}{45}\right) + 3.7$$
$$P_1(\beta) = -\left[0.2 + 0.0577\, sin\left(\frac{\pi\beta}{45}\right) + 2.1\right]$$

Hsieh and Lin [58] also gave three correlations (Eq. 13 - 19) based on the single-phase water side and the two-phase one for evaporation of R410A.

Single-phase water to water

$$h_w = 0.2092\left(\frac{k_l}{D_h}\right) Re^{0\cdot 78}\, Pr^{1/3}\left(\frac{u_m}{\mu_{wall}}\right)^{0\cdot 14} \tag{13}$$

For two-phase considering convective and nucleate boiling with $2000 < Re < 12000$, $0.0002 < Bo < 0.002$

$$h_r = E \cdot h_1 + S \cdot h_{pool} \tag{14}$$

Where,

$$h_l = 0.023 Re_l^{0\cdot 8} Pr^{0\cdot 4}\left(\frac{k_l}{D_h}\right) \tag{15}$$

$$h_{pool} = 55 P_r^{0.12} \cdot (-\,log_{10} P_r)^{-0.55} \cdot M^{-0.5} \cdot q^{0.67} \tag{16}$$

$$E = 1 + 24000 \cdot Bo^{1\cdot 16} + 1.37\left(\frac{1}{X_{tt}}\right)^{0.86} \tag{17}$$

$$S = (1 + 1.15 \times 10^{-6} E^2 Re_l^{1\cdot 17})^{-1} \tag{18}$$

$$f = 23820 \cdot Re_{eq}^{-1.12} \tag{19}$$

Kuo et al. [59] gave the same correlation for single phase as Hsieh and Lin [58] and created a two-phase correlation (Eq. 20 - 23) valid for condensation of R410A as given below

$$f_{tp} = 21500 \cdot Re_{eq}^{-1\cdot 14} \cdot Bo^{-0.085} \tag{20}$$

$$h_r = h_{r\cdot l} \cdot [0 \cdot 25 \cdot Co^{-0\cdot 49} Fr_l^{0\cdot 25} + 75 Bo^{0.75}] \tag{21}$$

$$Co = \left(\frac{\rho_g}{\rho_l}\right) \cdot \left(\frac{1 - X_m}{X_m}\right)^{0\cdot 8} \tag{22}$$

$$Fr_l = \frac{G^2}{\rho_l^2 \cdot g \cdot D_h} \tag{23}$$

Jain et al. [13] gave the following correlation (Eq. 25) which is valid for $Re < 2000$

$$Nu = 0.448 \times Re^{0.626} \times Pr^{0.4} \tag{24}$$

Dović and Švaić [12] gave a Colburn factor to friction factor ratio from the experiments conducted.

$$\frac{j}{f} = \frac{Nu p_r^{-1/3}}{f \cdot Re} = \frac{1}{A_c^2}\left[\frac{\dot{m}\alpha A Pr^{2/3}}{2\rho c_p \Delta p}\right] \tag{26}$$

Fernandes et al. [34] gave the correlation for the tortuosity factor as a result of the study

$$\tau = 1 + 0.5\sqrt{\left(\frac{1}{sin\,\beta}\right)^{\gamma} - 1} \tag{27}$$

$$K_0 = 16\left(\frac{90}{\beta}\right)^{0.6554 - 0.0929\gamma} \tag{28}$$

Khan et al. [35] used the combination of different angled plates and gave the correlations from the results as

For $\beta = 30°/30°$; $\beta = 60°/60°$; $\beta = 30°/60°$; $500 < Re < 2500$

$$Nu = \left(0.0161\frac{\beta}{\beta_{max}} + 0.1298\right) Re^{\left(0.198\frac{\beta}{\beta_{max}}+0.6398\right)} Pr^{0.35} \left(\frac{\mu}{\mu_w}\right)^{0.14} \quad (29)$$

Kumar et al. [30] gave a few correlations with the value of constants changing with each combination of *Re* and chevron angle. This correlation has been used to validate some of the experimental as well as numerical studies after it was published.

$$Nu = C_h . Re^n . Pr^{0.33} . (\frac{\mu}{\mu_w})^{0.17} \quad (30)$$

$$f = \frac{K_p}{Re^m} \quad (31)$$

Longo published numerous correlations as he has worked with different refrigerants. Using all the data he had collected over the years, a couple of correlations for boiling [74] as well as condensation [75] have been formulated.

$$h_w = 0.277(\lambda_w/d_h)\, Re^{0.766}\, Pr^{0.33} \quad (32)$$

$$\Delta p_c = 1.5G^{\,2}/_{2\rho_m} \quad (33)$$

$$\rho_m = \left[X_m/\rho_g + (1 - X_m)/\rho_L\right]^{-1} \quad (34)$$

For nucleate boiling

$$h_{nb} = C_{nb}\phi h_0 C_{Ra} F(p^*)(q\ /\ q^0)^n \quad (35)$$

For film condensation

$$h_{fc} = 1.875\phi\left(^{\lambda_L}/_{d_h}\right) \cdot Re_{eq}^{0.445} \cdot Pr_L^{1/3} \quad (36)$$

$$h_{sup} = h_{sat} + F\left[h_{s-ph} + c_{pG} q_{Lat}/\Delta J_{LG}\right] \quad (37)$$

Han et al. [18] gave the correlation (Eq.38 and 39) for *Nu* and *f* based on R 410A as the working fluid

$$Nu = Ge_1 Re_{Eq}^{Ge_2} \cdot Bo_{Eq}^{0.3} \cdot Pr^{0.4} \quad (38)$$

$$f = Ge_3 \cdot Re_{Eq}^{Ge_4} \quad (39)$$

Where,

$$Ge_1 = 2.81\left(\frac{p_{co}}{D_h}\right)^{-0.041} \cdot \left(\frac{\pi}{2} - \beta\right)^{-2.83}$$
$$Ge_2 = 0.746\left(\frac{p_{co}}{D_h}\right)^{-0.082} \cdot \left(\frac{\pi}{2} - \beta\right)^{0.61}$$
$$Ge_3 = 64710\left(\frac{p_{co}}{D_h}\right)^{-5.27} \cdot \left(\frac{\pi}{2} - \beta\right)^{-3.03}$$
$$Ge_4 = -1.314\left(\frac{p_{co}}{D_h}\right)^{-0.62} \cdot \left(\frac{\pi}{2} - \beta\right)^{-0.47}$$

Desideri et al. [24] gave the correlation (Eq. 40 and 41) of heat transfer coefficient and pressure drop for evaporation of R245fa and HFO- 1233zd in *BPHE* for ORC systems

$$h = 1.48e3 \cdot We^{-3.22e2} \cdot (\rho^*)^{-3.38e-1} \cdot Re_l^{4.51e-1} \cdot Bd^{-4.69e-1} \quad (40)$$

Table 2. Constant values for Kumar et al. [30] correlation

Angle (degrees)	Heat transfer			Pressure Loss		
	Re	*Ch*	*n*	*Re*	*Kp*	*m*
≤30°	≤10	0.718	0.349	<10	50	1
	>10	0.348	0.663	10-100	19.4	0.589
				>100	2.99	0.183
45°	<10	0.718	0.349	<15	47	1
	10-100	0.4	0.598	15-300	18.29	0.652
	>100	0.3	0.663	>300	1.441	0.206
60°	<20	0.562	0.326	<40	24	1
	20-400	0.306	0.529	40-400	3.24	0.457
	>400	0.108	0.703	>400	0.76	0.215
≥65°	<20	0.562	0.326	<50	24	1
	20-500	0.331	0.503	50-500	2.8	0.451
	>500	0.087	0.718	>500	0.639	0.213

$$\Delta p_{fric} = 138\frac{G^2}{2 \cdot \rho_m} \quad (41)$$

Where,

$$We = \frac{G^2 \cdot d_h}{\rho_m \theta}$$

$$B_0 = \frac{\dot{q}}{G \Delta h_{vap}}$$

$$Bd = \frac{(\rho_l - \rho_v) \cdot g \cdot d_h^2}{\theta}$$

Imran et al. [101] gave two correlations each for *Nu* and *f* for $\beta = 45°$ *and* $\beta = 60°$, for R245fa's flow boiling in *BPHE* for ORC systems

For $\beta = 45°$

$$Nu_{tp} = 3.61 \cdot Re_{eq}^{2.384} \cdot Bo_{eq}^{1.321} \cdot We^{-0.229} \cdot Bd^{-0.76} \quad (42)$$

$$f_{tp} = 1.37 \cdot Re_{eq}^{-0.0611} \cdot Bo_{eq}^{0.045} \cdot We^{-0.64} \cdot Bd^{0.0375} \quad (43)$$

For $\beta = 60°$

$$Nu_{tp} = 5.89 \cdot Re_{eq}^{2.905} \cdot Bo_{eq}^{1.568} \cdot We^{-0.6087} \cdot Bd^{0.985} \quad (44)$$

$$f_{tp} = 2.57 \cdot Re_{eq}^{-0.246} \cdot Bo_{eq}^{1.568} \cdot We^{-0.3716} \cdot Bd^{0.0815} \quad (45)$$

Shon et al., gave correlation (Eq. 46 and 47) for *f* and *Nu* for condensation of R1233zd(E).

For $500 < Re_{eq} < 2500$, $4.8 < Pr_l < 5.3$

$$Nu = 2.337 \cdot Re_{eq}^{1.024} \cdot Re_{lo}^{-0.294} \cdot Bo_{eq}^{0.361} \cdot Pr_l^{0.333} \quad (46)$$

Where, $Re_{lo} = \frac{GD_h}{\mu_l}$

For $500 < Re_{eq} < 2500$, $130 < Pr_l < 250$

$$f = 1261.067 Re_{eq}^{-0.411} Re_{lo}^{-0.57} \quad (47)$$

Lee et al. [111] also gave a correlation for f and *Nu* for evaporation of R-1233zd(E) [104] and R-1234ze(E)/R32

$$Nu_r = 0.9243 \cdot Re_{eq}^{0.6151} \cdot Pr_l^{0.33} \quad (48)$$

$$f_{tp} = 6.25 \times 10^{-4} \cdot Re_{eq}^{1.427} \cdot Re_l^{-0.7098} \cdot Pr_l^{0.4036} \quad (49)$$

CONCLUSION

In conclusion, the extensive research conducted on *BPHE* has provided valuable insights into their performance across various operating conditions and applications. Studies on single-phase flows have shed light on the influence of geometric parameters, such as chevron angles, on heat transfer and pressure drop characteristics. Additionally, investigations into two-phase flows, particularly involving refrigerant evaporation and condensation, have resulted in the formulation of correlations for friction factor and Nusselt number, aiding in the design and optimization of *BPHE*s. Moreover, numerical studies using *CFD* have allowed for detailed analyses of flow and heat transfer patterns, albeit at a high computational cost. These studies have collectively contributed to a deeper understanding of *BPHE*s, their potential applications in systems like Organic Rankine cycles, and the challenges associated with their design and optimization. Overall, the research efforts in single-phase, two-phase, and numerical studies have significantly advanced the field of brazed plate heat exchangers, paving the way for further innovations and improvements in their performance and efficiency. The following conclusions were the findings on the advancement in the research of brazed plate heat exchangers.

- Flow and heat transfer patterns have been primarily investigated in gasketed plate heat exchangers, but their findings are applicable to brazed plate heat exchangers due to their similar geometry.
- Studies on single-phase flows are comparatively limited, with a focus on variations in chevron angles as the most common investigation.
- Two-phase flow studies predominantly involve refrigerant evaporation and condensation, leading to the formulation of correlations for friction factor (*f*) and Nusselt number (*Nu*) based on extensive databases. However, differences in operating conditions and correlation techniques have resulted in multiple correlations for similar refrigerants.
- *BPHE*s have found applications in Organic Rankine cycle systems as evaporators and with nanofluid applications. However, the impact of nanofluids on heat transfer in *BPHE*s appears less significant compared to other types of heat exchangers.

Computational fluid dynamics *(CFD)* studies remain essential but computationally expensive due to the complex geometries of *BPHE*s, necessitating the use of a large number of elements and computational resources.

NOMENCLATURE

Bo	Boiling Number
d	Diameter
f	Friction factor
G	Mass flux
g	Acceleration due to gravity
h	Heat transfer coefficient
ΔJ_{LG}	Enthalpy of vaporization
L	Length
Nu	Nusselt number
Pr	Prandtl number

p	pressure
p_{cr}	Critical pressure
q	Heat flux
Re	Reynolds number
R_p	Roughness
R_a	Average mean roughness
ΔT	Temperature difference
u	Average velocity
X	Vapor quality
X_{tt}	Martinelli Parameter

Other Symbols

ρ	Density
ϕ	Area enlargement factor
β	Chevron angle
μ	Viscosity
λ	Thermal conductivity

Subscripts

cb	Convective boiling
eq	Equivalent
fc	Forced convection
g	Gaseous phase
G	Saturated vapor
h	Hydraulic
l	Liquid phase
L	Saturated liquid
Lat	Latent
m	Mean
nb	Nucleate boiling
r	refrigerant
sat	Saturated
s	Superheated
tp	Two-phase
0	Reference state

AUTHORSHIP CONTRIBUTIONS

Authors equally contributed to this work.

DATA AVAILABILITY STATEMENT

The authors confirm that the data that supports the findings of this study are available within the article. Raw data that support the finding of this study are available from the corresponding author, upon reasonable request.

CONFLICT OF INTEREST

The author declared no potential conflicts of interest with respect to the research, authorship, and/or publication of this article.

ETHICS

There are no ethical issues with the publication of this manuscript.

REFERENCES

[1] Ribeiro CP, Caño Andrade MH. An algorithm for steady-state simulation of plate heat exchangers. J Food Engineer 2002;53:59-66. [CrossRef]

[2] Butt AG, inventor; USPTO. Pate type heat exchanger and method of construction and repair. US3372453A, patent. 1968.

[3] Thonon B. Design method for plate evaporators and condensers. 1st Int Conf Process Intensif Chem Ind 1995:37-45.

[4] Focke WW, Zachariades J, Olivier I. The effect of the corrugation inclination angle on the thermohydraulic performance of plate heat exchangers. Int J Heat Mass Transf 1985;28:1469-1479. [CrossRef]

[5] Shah RK, Sekulic DP. Fundamentals of Heat Exchanger Design. New Jersey: John Wiley Sons; 2003. [CrossRef]

[6] Allison J, inventor; India. Plate heat exchanger. IN154238B, patent. 1985.

[7] Fuerschbach RF, Creighton TP, Fijas DF, inventors; European Patent Office. Plate type heat exchanger. 89201312.9, patent application. 1989.

[8] Yam YY, Lin TF, Yang BC. Evaporation heat transfer and pressure drop of refrigerant R134a in a plate heat exchanger. Proc ASME Turbo Expo 1997;121.

[9] William TG, Glen Hubman GC, inventors; USPTO. Brazed plate heat exchanger utilizing metal gaskets and method for making same. US0030043 A1, patent. 2001.

[10] Heil D, Bruno Metzel K, Schwab E, Alois Tischler MW, inventors; USPTO. Plate heat exchanger and method of making same. US 6,389,696 B1, patent. 2002.

[11] Grijspeerdt K, Hazarika B, Vucinic D. Application of computational fluid dynamics to model the hydrodynamics of plate heat exchangers for milk processing. J Food Engineer 2003;57:237-242. [CrossRef]

[12] Dović D, Švaić S. Influence of chevron plates geometry on performances of plate heat exchangers. Teh Vjesn 2007;14:37-45.

[13] Jain S, Joshi A, Bansal PK. A new approach to numerical simulation of small sized plate heat exchangers with chevron plates. J Heat Transf 2007;129:291-297. [CrossRef]

[14] Otahal K, Hofer J, inventors; USPTO. Plate heat exchanger having a turbulence generator. US 8,418,752 B2, patent. 2013.

[15] Krantz J, inventor; USPTO. Plate structure and gasket for a heat exchanger. US 9.212,854 B2, patent. 2015.

[16] Bogaert R, Böles A. Global performance of a prototype brazed plate heat exchanger in a large reynolds number range. Exp Heat Transf 1995;8:293-311. [CrossRef]

[17] Palmer SC, Payne WV, Domanski P. Evaporation and condensation heat transfer performance of flammable refrigerants in a brazed plate heat exchanger. NIST Interagency/Internal Rep 2000:6541. [CrossRef]
[18] Han DH, Lee KJ, Kim YH. Experiments on the characteristics of evaporation of R410A in brazed plate heat exchangers with different geometric configurations. Appl Therm Engineer 2003;23:1209-1225. [CrossRef]
[19] Gullapalli VS. Estimation of thermal and hydraulic characteristics of compact brazed plate heat exchangers (dissertation). Lund University; 2013. [CrossRef]
[20] Gullapalli VS, Sundén B. Cfd simulation of heat transfer and pressure drop in compact brazed plate heat exchangers. Heat Transf Engineer 2014;35:358-366. [CrossRef]
[21] Gullapalli V, Lic T. Design of high efficiency compact brazed plate heat exchangers (BPHE) using CFD. 23rd IIR International Congress of Refrigeration, Prague, 614; 2011. pp.1-11.
[22] Barzegarian R, Moraveji MK, Aloueyan A. Experimental investigation on heat transfer characteristics and pressure drop of BPHE (brazed plate heat exchanger) using TiO2-water nanofluid. Exp Therm Fluid Sci 2016;74:11-18. [CrossRef]
[23] Teng TP, Hsiao TC, Chung CC. Characteristics of carbon-based nanofluids and their application in a brazed plate heat exchanger under laminar flow. Appl Therm Engineer 2019;146:160-168. [CrossRef]
[24] Desideri A, Zhang J, Kærn MR, Ommen TS, Wronski J, Lemort V, et al. An experimental analysis of flow boiling and pressure drop in a brazed plate heat exchanger for organic Rankine cycle power systems. Int J Heat Mass Transf 2017;113:6-21. [CrossRef]
[25] Kim DY, Kim KC. Thermal performance of brazed metalfoam-plate heat exchanger as an evaporator for organic Rankine cycle. Energy Procedia 2017;129:451-458. [CrossRef]
[26] Nematollahi O, Abadi GB, Kim DY, Kim KC. Experimental study of the effect of brazed compact metal-foam evaporator in an organic Rankine cycle performance: Toward a compact ORC. Energy Conver Manage 2018;173:37-45. [CrossRef]
[27] Kandlikar SG, Shah RK. Asymptotic effectiveness-NTU formulas for multipass plate heat exchangers. ASME 1989;111:315-321. [CrossRef]
[28] Galeazzo FCC, Miura RY, Gut JAW, Tadini CC. Experimental and numerical heat transfer in a plate heat exchanger. Chem Engineer Sci 2006;61:7133-7138. [CrossRef]
[29] Muley A, Manglik RM. Experimental study of turbulent flow heat transfer and pressure drop in a plate heat exchanger with chevron plates. J Heat Transf 1999;121:110-117. [CrossRef]
[30] Kumar H. The plate heat exchanger: Construction and design. Institute Chem Engineer Symposium Series 1984;86:1275-1288. [CrossRef]
[31] Blomerius H, Mitra NK. Numerical investigation of convective heat transfer and pressure drop in wavy ducts. Numer Heat Transf Part A Appl 2000;37:37-54. [CrossRef]
[32] Kanaris AG, Mouza AA, Paras S V. Optimal design of a plate heat exchanger with undulated surfaces. Int J Therm Sci 2009;48:1184-95. [CrossRef]
[33] Han W, Saleh K, Aute V, Ding G, Hwang Y, Radermacher R. Numerical simulation and optimization of single-phase turbulent flow in chevron-type plate heat exchanger with sinusoidal corrugations. HVAC R Res 2011;17:186-197. [CrossRef]
[34] Fernandes CS, Dias RP, Nóbrega JM, Maia JM. Laminar flow in chevron-type plate heat exchangers: CFD analysis of tortuosity, shape factor and friction factor. Chem Engineer Process Process Intensif 2007;46:825-833. [CrossRef]
[35] Khan TS, Khan MS, Chyu MC, Ayub ZH. Experimental investigation of single phase convective heat transfer coefficient in a corrugated plate heat exchanger for multiple plate configurations. Appl Therm Engineer 2010;30:1058-1065. [CrossRef]
[36] Manigandan N, Naveenprabhu V, Suresh ML. Experimental investigation of a brazed chevron type plate heat exchanger. Int J Sci Technol Engineer 2015;1:1-7.
[37] Gurel B, Akkaya VR, Goltas M, Sen CN, Guler OV, Kosar MI, et al. Investigation on flow and heat transfer of compact brazed plate heat exchanger with lung pattern. Appl Therm Engineer 2020;175:115309. [CrossRef]
[38] Fernández-Seara J, Diz R, Uhía FJ. Pressure drop and heat transfer characteristics of a titanium brazed plate-fin heat exchanger with offset strip fins. Appl Therm Engineer 2013;51:502-511. [CrossRef]
[39] Cremaschi L, Spitler JD, Lim E, Ramesh A. Waterside fouling performance in brazed-plate-type condensers for cooling tower applications. HVAC R Res 2011;17:198-217. [CrossRef]
[40] Kim MB, Park CY. An experimental study on single phase convection heat transfer and pressure drop in two brazed plate heat exchangers with different chevron shapes and hydraulic diameters. J Mech Sci Technol 2017;31:2559-2571. [CrossRef]
[41] Jin S, Hrnjak P. Effect of end plates on heat transfer of plate heat exchanger. Int J Heat Mass Transf 2017;108:740-748. [CrossRef]
[42] Li W, Hrnjak P. Compensating for the end-plate effect on heat transfer in brazed plate heat exchangers. Int J Refrig 2021;126:99-108. [CrossRef]
[43] Wu J, Ju Y. Comprehensive comparison of small-scale natural gas liquefaction processes using brazed plate heat exchangers. Front Energy 2020;14:683-698. [CrossRef]

[44] Zhong Y, Deng K, Zhao S, Hu J, Zhong Y, Li Q, et al. Experimental and numerical study on hydraulic performance of chevron brazed plate heat exchanger at low Reynolds number. Processes 2020;8:1076. [CrossRef]
[45] Jafari A, Sadeghianjahromi A, Wang CC. Experimental and numerical investigation of brazed plate heat exchangers - A new approach. Appl Therm Engineer 2022;200:117694. [CrossRef]
[46] Ham J, Yong J, Kwon O, Bae K, Cho H. Experimental investigation on heat transfer and pressure drop of brazed plate heat exchanger using LiBr solution. Appl Therm Engineer 2023;225:120161. [CrossRef]
[47] Fazeli I, Sarmasti Emami MR, Rashidi A. Investigation and optimization of the behavior of heat transfer and flow of MWCNT-CuO hybrid nanofluid in a brazed plate heat exchanger using response surface methodology. Int Comm Heat Mass Transf 2021;122:105175. [CrossRef]
[48] Mehrarad H, Sarmasti Emami MR, Afsari K. Thermal performance and flow analysis in a brazed plate heat exchanger using MWCNT@water/EG nanofluid. Int Comm Heat Mass Transf 2023;146:106867. [CrossRef]
[49] Gungor S. Experimental comparison on energy consumption and heat transfer performance of corrugated H-type and L-type brazed plate heat exchangers. Int Comm Heat Mass Transf 2023;144:106763. [CrossRef]
[50] Pulagam MKR, Rout SK, Sarangi SK. Numerical simulation of a brazed plate heat exchanger using Al2O3-water nanofluid with periodic boundary conditions. WSEAS Trans Heat Mass Transf 2023;18:262-270. [CrossRef]
[51] Jalili B, Aghaee N, Jalili P, Domiri Ganji D. Novel usage of the curved rectangular fin on the heat transfer of a double-pipe heat exchanger with a nanofluid. Case Stud Therm Engineer 2022;35:102086. [CrossRef]
[52] Jalili P, Kazerani K, Jalili B, Ganji DD. Investigation of thermal analysis and pressure drop in non-continuous helical baffle with different helix angles and hybrid nano-particles. Case Stud Therm Engineer 2022;36:102209. [CrossRef]
[53] Kaplan S, Bayramoğlu K, Sarikanat M, Altay L. Numerical study on heat transfer and fluid dynamics in plate heat exchangers: Effects of chevron angle and aspect ratio. J Therm Engineer 2024;10:638-656. [CrossRef]
[54] Bousri A, Hamadouche A, Khali S, Nebbali R, Beji H. Forced convection coolig of multiple heat sources using open cell metal foams. J Therm Engineer 2021;7:255-270. [CrossRef]
[55] Aouanouk SA, Mouheb A, Absi R. Numerical study of milk fouling thickness in the channel of plate heat exchanger. J Therm Engineer 2018;4:2464-2470. [CrossRef]
[56] Zhu CX, Wang CC, Tang YC. Performance and flow distribution of the plate heat exchanger with supercritical fluid of carbon dioxide. J Therm Engineer 2015;1:143-151. [CrossRef]
[57] Yan YY, Lio HC, Lin TF. Condensation heat transfer and pressure drop of refrigerant R-134a in a plate heat exchanger. Int J Heat Mass Transf 1999;42:993-1006. [CrossRef]
[58] Hsieh YY, Lin TF. Evaporation heat transfer and pressure drop of refrigerant R-410A flow in a vertical plate heat exchanger. J Heat Transf 2003;125:852-857. [CrossRef]
[59] Kuo WS, Lie YM, Hsieh YY, Lin TF. Condensation heat transfer and pressure drop of refrigerant R-410A flow in a vertical plate heat exchanger. Int J Heat Mass Transf 2005;48:5205-5220. [CrossRef]
[60] Longo GA, Gasparella A. HFC-410A vaporisation inside a commercial brazed plate heat exchanger. Exp Therm Fluid Sci 2007;32:107-116. [CrossRef]
[61] Longo GA. R410A condensation inside a commercial brazed plate heat exchanger. Exp Therm Fluid Sci 2009;33:284-291. [CrossRef]
[62] Palm B, Claesson J. Plate heat exchangers: Calculation methods for singleand two-phase flow. Heat Transf Eng 2006;27:88-98. [CrossRef]
[63] Longo GA, Gasparella A. Refrigerant R134a vaporisation heat transfer and pressure drop inside a small brazed plate heat exchanger. Int J Refrig 2007;30:821-830. [CrossRef]
[64] Longo GA. Refrigerant R134a condensation heat transfer and pressure drop inside a small brazed plate heat exchanger. Int J Refrig 2008;31:780-789. [CrossRef]
[65] Longo GA, Gasparella A. Heat transfer and pressure drop during HFC refrigerant vaporisation inside a brazed plate heat exchanger. Int J Heat Mass Transf 2007;50:5194-5203. [CrossRef]
[66] Longo GA, Mancin S, Righetti G, Zilio C. Hydrocarbon refrigerants condensation local heat transfer coefficients inside a brazed plate heat exchanger (BPHE). Int J Heat Mass Transf 2023;201:123615. [CrossRef]
[67] Longo GA, Mancin S, Righetti G, Zilio C. Hydrocarbon refrigerants boiling local heat transfer coefficients inside a brazed plate heat exchanger (BPHE). Int J Refrig 2023;156:113-122. [CrossRef]
[68] Longo GA. Heat transfer and pressure drop during HFC refrigerant saturated vapour condensation inside a brazed plate heat exchanger. Int J Heat Mass Transf 2010;53:1079-1087. [CrossRef]
[69] Longo GA. Heat transfer and pressure drop during hydrocarbon refrigerant condensation inside a brazed plate heat exchanger. Int J Refrig 2010;33:944-953. [CrossRef]
[70] Longo GA. The effect of vapour super-heating on hydrocarbon refrigerant condensation inside a brazed plate heat exchanger. Exp Therm Fluid Sci 2011;35:978-985. [CrossRef]

[71] Longo GA. Vaporisation of the low GWP refrigerant HFO1234yf inside a brazed plate heat exchanger. Int J Refrig 2012;35:952-961. [CrossRef]
[72] Longo GA, Zilio C, Righetti G, Brown JS. Condensation of the low GWP refrigerant HFO1234ze(E) inside a brazed plate heat exchanger. Int J Refrig 2014;38:250-259. [CrossRef]
[73] Longo GA, Mancin S, Righetti G, Zilio C. Boiling of the new low-GWP refrigerants R1234ze(Z) and R1233zd(E) inside a small commercial brazed plate heat exchanger. Int J Refrig 2019;104:376-385. [CrossRef]
[74] Longo GA, Mancin S, Righetti G, Zilio C. A new model for refrigerant boiling inside brazed plate heat exchangers (BPHEs). Int J Heat Mass Transf 2015;91:144-149. [CrossRef]
[75] Longo GA, Righetti G, Zilio C. A new computational procedure for refrigerant condensation inside herringbone-type brazed plate heat exchangers. Int J Heat Mass Transf 2015;82:530-536. [CrossRef]
[76] Longo GA, Zilio C, Righetti G. Condensation of the low GWP refrigerant HFC152a inside a brazed plate heat exchanger. Exp Therm Fluid Sci 2015;68:509-515. [CrossRef]
[77] Longo GA, Mancin S, Righetti G, Zilio C. Local heat transfer coefficients of R32 and R410A boiling inside a brazed plate heat exchanger (BPHE). Appl Therm Engineer 2022;215:118930. [CrossRef]
[78] Longo GA, Mancin S, Righetti G, Zilio C. HFC404A vaporisation inside a brazed plate heat exchanger (BPHE): Comparison with the possible long-term low GWP substitutes HC290 (Propane) and HC1270 (Propylene). Appl Therm Engineer 2016;108:1401-1408. [CrossRef]
[79] Longo GA, Mancin S, Righetti G, Zilio C. Boiling of the new low-GWP refrigerants R1234ze(Z) and R1233zd(E) inside a small commercial brazed plate heat exchanger. Int J Refrig 2019;104:376-385. [CrossRef]
[80] Longo GA, Mancin S, Righetti G, Zilio C. Local heat transfer coefficients of R32 and R410a condensation inside a brazed plate heat exchanger (BPHE). Int J Heat Mass Transf 2022;194:123041. [CrossRef]
[81] Claesson J. Correction of logarithmic mean temperature difference in a compact brazed plate evaporator assuming heat flux governed flow boiling heat transfer coefficient. Int J Refrig 2005;28:573-578. [CrossRef]
[82] Hayes N, Jokar A, Ayub ZH. Study of carbon dioxide condensation in chevron plate exchangers; Pressure drop analysis. Int J Heat Mass Transf 2012;55:2916-2925. [CrossRef]
[83] Muthuraman S. The characteristics of brazed plate heat. Glob J Res Engineer Mech Mech Engineer 2011;11:11-26.
[84] Mancin S, Del Col D, Rossetto L. R32 partial condensation inside a brazed plate heat exchanger. Int J Refrig 2013;36:601-611. [CrossRef]
[85] Rossato M, Del Col D, Muzzolon A, Rossetto L. Flow boiling of R32 inside a brazed plate heat exchanger. Int J Refrig 2016;69:165-174. [CrossRef]
[86] Pang W, Liu J, He J, Xu X. Thermal performance of brazed plate heat exchangers for a mixed-refrigerant Joule-Thomson cooler. Int J Refrig 2016;61:37-54. [CrossRef]
[87] Raveendran PS, Sekhar SJ. Experimental studies on domestic refrigeration system with brazed plate heat exchanger as condenser. J Mech Sci Technol 2016;30:2865-2871. [CrossRef]
[88] Táboas F, Vallès M, Bourouis M, Coronas A. Flow boiling heat transfer of ammonia/water mixture in a plate heat exchanger. Int J Refrig 2010;33:695-705. [CrossRef]
[89] Mutumba A, Coletti F, Reip A, Mahmoud MM, Karayiannis TG. Experiments and correlations for single-phase convective heat transfer in brazed plate heat exchangers. Heat Transf Engineer 2023;44:211-231. [CrossRef]
[90] Li W, Hrnjak P. Visualization of two-phase refrigerant flow in the inlet header of brazed plate heat exchangers and its effect on distribution. Int J Refrig 2021;131:483-492. [CrossRef]
[91] Li W, Hrnjak P. Quantification of two-phase refrigerant distribution in brazed plate heat exchangers using infrared thermography. Int J Refrig 2021;131:348-358. [CrossRef]
[92] Li W. Flow distribution in brazed plate heat exchangers (dissertation). Urbana, Illinois; University of Illinois at Urbana-Champaign; 2021.
[93] Navarro-Peris E, Alvarez-Piñeiro L, Schnabel L, Corberan JM. Refrigerant maldistribution in brazed plate heat exchanger evaporators. Part B: Analysis of the influence of maldistribution on the evaporator performance. Int J Refrig 2021;131:312-321. [CrossRef]
[94] Li W, Hrnjak P. Single-phase flow distribution in plate heat exchangers: Experiments and models. Int J Refrig 2021;126:45-56. [CrossRef]
[95] Li W, Hrnjak P. Modeling of two-phase refrigerant distribution in brazed plate heat exchangers. Int J Refrig 2022;136:172-183. [CrossRef]
[96] Will T, Schnabel L, Köhler J. Detailed thermal evaluation of brazed plate heat exchanger using infrared thermography. Chemie-Ingenieur-Technik 2023;95:732-739. [CrossRef]
[97] Zendehboudi A, Ye Z, Hafner A, Andresen T, Skaugen G. Heat transfer and pressure drop of supercritical CO2 in brazed plate heat exchangers of the tri-partite gas cooler. Int J Heat Mass Transf 2021;178:121641. [CrossRef]
[98] Sadeghianjahromi A, Jafari A, Wang CC. Numerical investigation of the effect of chevron angle on thermofluids characteristics of non-mixed and mixed brazed plate heat exchangers with experimental validation. Int J Heat Mass Transf 2022;184:122278. [CrossRef]

[99] Salman M, Prabakaran R, Kumar PG, Lee D, Kim SC. Saturation flow boiling characteristics of R290 (propane) inside a brazed plate heat exchanger with offset strip fins. Int J Heat Mass Transf 2023;202:123778. [CrossRef]
[100] Gullapalli VS. Modeling of brazed plate heat exchangers for ORC systems. Energy Procedia 2017;129:443-450. [CrossRef]
[101] Imran M, Usman M, Yang Y, Park BS. Flow boiling of R245fa in the brazed plate heat exchanger: Thermal and hydraulic performance assessment. Int J Heat Mass Transf 2017;110:657-670. [CrossRef]
[102] Wu J, He T, Ju Y. Experimental study on CO2 frosting and clogging in a brazed plate heat exchanger for natural gas liquefaction process. Cryogenics (Guildf) 2018;91:128-135. [CrossRef]
[103] Shon BH, Jung CW, Kwon OJ, Choi CK, Tae Kang Y. Characteristics on condensation heat transfer and pressure drop for a low GWP refrigerant in brazed plate heat exchanger. Int J Heat Mass Transf 2018;122:1272-1282. [CrossRef]
[104] Lee DC, Kim D, Park S, Lim J, Kim Y. Evaporation heat transfer coefficient and pressure drop of R-1233zd(E) in a brazed plate heat exchanger. Appl Therm Engineer 2018;130:1147-1155. [CrossRef]
[105] Kho T, Müller-Steinhagen H. An experimental and numerical investigation of heat transfer fouling and fluid flow in flat plate heat exchangers. Chem Engineer Res Des 1999;77:124-130. [CrossRef]
[106] Grigore R, Popa S, Hazi A, Hazi G. Research about correlation between the performance of plate heat exchanger and the number of plates. Proc 3rd WSEAS Int Conf Finite Differ - Finite Elem - Finite Vol - Bound Elem F-and-B '10 2010:92-97.
[107] Sundén B. Computational fluid dynamics in research and design of heat exchangers. Heat Transf Engineer 2007;28:898-910. [CrossRef]
[108] Sevilgen G, Bayram H. Numerical analysis of heat transfer of a brazed plate heat exchanger. Acad Platf J Engineer Sci 2020;8:491-499.
[109] Lonis F, Luo Y, Andresen J, Maroto-Valer M. Capture of cold energy from liquid nitrogen using a brazed plate heat exchanger. Energy Procedia 2019;158:5622-5628. [CrossRef]
[110] Martin H. A theoretical approach to predict the performance of chevron-type plate heat exchangers. Chem Engineer Process Process Intensif 1996;35:301-310. [CrossRef]
[111] Lee DC, Kim D, Cho W, Kim Y. Evaporation heat transfer and pressure drop characteristics of R1234ze(E)/R32 as a function of composition ratio in a brazed plate heat exchanger. Int J Heat Mass Transf 2019;140:216-226. [CrossRef]